Biophysical characterization and single-chain Fv construction of a neutralizing antibody to measles virus

Takashi Tadokoro[1], Mst Lubna Jahan[1], Yuri Ito[1], Maino Tahara[2], Surui Chen[1], Atsutoshi Imai[1], Natsumi Sugimura[1], Koki Yoshida[1], Mizuki Saito[1], Toyoyuki Ose[1], Takao Hashiguchi[3], Makoto Takeda[2], Hideo Fukuhara[1], Katsumi Maenaka[1,*]

[1] Faculty of Pharmaceutical Science, Hokkaido University, Sapporo, Japan.
[2] Department of Virology 3, National Institute of Infectious Diseases, Tokyo, Japan
[3] Department of Virology, Faculty of Medicine, Kyushu University, Fukuoka, Japan

* Corresponding author; Katsumi Maenaka (maenaka@pharm.hokudai.ac.jp)

Running title: *Characterization of a measles neutralizing antibody*

Abbreviations; scFv, single-chain fragment variable; mAb, monoclonal antibody; CDR, complementarity determining region; MV, measles virus; SPR, surface plasmon resonance; DSC, differential scanning calorimetry;

Keywords; Measles virus, hemagglutinin, single-chain fragment variables, neutralizing antibody, SLAM, Nectin-4, surface plasmon resonance

Abstract

The measles virus (MV) is a major cause of childhood morbidity and mortality worldwide. We previously established a mouse monoclonal antibody, 2F4, which shows high neutralizing titers against 8 different genotypes of MV. However, the molecular basis for the neutralizing activity of the 2F4 antibody remains incompletely understood. Here, we have evaluated the binding characteristics of a Fab fragment of the 2F4 antibody. Using the MV infectious assay, we demonstrated that 2F4 Fab inhibits viral entry via either of two cellular receptors, SLAM and Nectin4. Surface plasmon resonance (SPR) analysis of recombinant proteins indicated that 2F4 Fab interacts with MV hemagglutinin (MV-H) with a K_D value at the nM level. Furthermore, we designed a single-chain Fv fragment of 2F4 antibody as another potential biopharmaceutical to target measles. The stable 2F4 scFv was successfully prepared by the refolding method and shown to interact with MV-H at the μM level. Like 2F4 Fab, scFv inhibited receptor binding and viral entry. This indicates that 2F4 mAb uses the receptor-binding site and/or a neighboring region as an epitope with high affinity. These results provide insight into the neutralizing activity and potential therapeutic use of antibody fragments for MV infection.

Introduction

Measles is one of the leading causes of death among children, especially under the age of 5 even though a safe and cost-effective vaccine is available [1]. In 2012, the World Health Organization (WHO) Global Vaccine Action Plan stated a goal for measles elimination in 5 of the 6 WHO regions by 2020. Nonetheless, the WHO reported that approximately 89,780 people died from measles globally in 2016 (http://www.who.int/mediacentre/factsheets/fs286/). According to the Centers for Disease Control and Prevention (CDC), the United States experienced a measles outbreak, including 189 infected people in 2015 (http://www.cdc.gov/). Thus, measles virus (MV) infections remain a feasible threat to global health. MV belongs to the genus *Morbillivirus* of the family *Paramyxoviridae* [2, 3]. MV is an RNA virus with a negative-strand RNA genome, which encodes genes for nucleocapsid (N) protein, Large (L) protein, phospho (P) protein, matrix (M) protein, hemagglutinin (H), fusion (F) protein and nonstructural proteins (C and V). MV infection is initiated by binding of the H protein to cellular receptors on the host target cells and the binding triggers membrane fusion between the virus envelope and the host cell plasma membrane, mediated by the F protein. The signaling lymphocyte activation molecule (SLAM) on a subset of immune cells and Nectin-4 at adherens junctions are identified as the major receptors for MV [4-6]. Since H and F proteins, viral envelope glycoproteins, are involved in the MV entry to the host cells [7, 8], they both become neutralizing targets.

To date, a large number of neutralizing antibodies (Abs) have been elicited against the viral envelope glycoproteins, MV-H and MV-F, mainly the MV-H protein [9-12]. We have previously isolated and characterized a monoclonal antibody (mAb), 2F4 that shows high neutralizing titers against 8 different genotype MV strains [13]. The results suggest that the epitope of mAb 2F4 are overlapped with and/or close to the binding site of the receptors, although the epitopes have not been completely determined yet. Structural studies have suggested that all the cellular receptors, including SLAM and Nectin-4 largely shared the binding region on the MV-H protein [14-17]. Since both SLAM and Nectin-4 binding to MV-H are relevant for MV pathogenesis, escape from immune surveillance by mutations on the site should not occur in nature due to the high probability to lose the receptor binding ability.

mAb becomes one of the most popular therapeutic tools, including viral neutralization [18, 19]. However, intact antibodies have large molecular size and sometimes show high levels of immunogenicity. In addition, their production is poorly economical. Hence, small antibody fragments have recently been used as alternatives to monoclonal antibodies in therapeutic applications [20, 21]. The most popular types of recombinant antibodies include Fab fragment and single-chain fragment variables (scFvs). The Fab fragments can be easily obtained from intact full antibody by digestion of protease, such as papain to remove the crystallized fragment (Fc). On the other hand, the scFv consists of variable heavy (V_H) and variable light (V_L) domains linked by a flexible polypeptide linker. The scFv has its small molecular size which enables better tissue penetration and its lower level of immunogenicity. The advantages in the use of scFv are (1) easy modification using gene manipulation technique, and (2) low-cost production, such as the *E. coli* expression system.

Here, we have prepared the Fab fragment of 2F4 mAb to exclude the effect of its Fc fragment for MV infection. The surface plasmon resonance (SPR) analysis revealed that 2F4 Fab binds to MV-H with the dissociation constant of 18 ± 3 nM and competes with the MV-H binding of cellular receptors, SLAM and Nectin-4. We have further constructed the single chain fragment variable of 2F4 mAb. The SPR analysis demonstrated that 2F4-scFv can bind to the MV-H ectodomain with low μM of K_D but can inhibit cellular receptor (SLAM and Nectin-4) binding to MV-H protein. Our findings reveal that 2F4 mAb recognizes the receptor binding regions as an epitope and provide insight into the rational design of fragmented antibody for MV neutralization.

Results

To investigate the molecular basis of the interaction between the 2F4 Fab fragment and MV-H, we prepared 2F4 mAb and 2F4 Fab fragments (Fig.1A). To clarify whether 2F4 Fab can neutralize the MV infection, we performed a neutralizing assay using recombinant MV, which was based on the IC323 genomic background and encoded a *Renilla* luciferase reporter gene and a different genotype H gene [10, 13]. Consistent with the previous findings, the 2F4 mAb effectively neutralized the recombinant MV infection to both SLAM- and Nectin-4-expressing Vero cells, while the

2F4 Fab fragment sufficiently neutralized (Fig. 1B). The concentration for the 50% reduction of the infection against SLAM expressing Vero cells is estimated to be 0.2 nM for 2F4 mAb and 7 nM for 2F4 Fab, while those against Necitn-4 expressing Vero cells are 0.4 nM for 2F4 mAb and 6 nM for 2F4 Fab.

To understand the MV neutralization mechanism by Fab at the molecular level, we performed kinetic analysis for 2F4-Fab using SPR. The MV-H protein was prepared by transient expression in HEK293T cells (Fig. 2A). The binding affinity of 2F4-Fab to MV-H was calculated to be K_D = 18 ± 3 nM (Fig. 2B, Table 1). The association and dissociation kinetic constants (k_{on} and k_{off}) were $1.7 \pm 0.1 \times 10^5$ M^{-1} s^{-1} and $2.8 \pm 0.3 \times 10^{-3}$ s^{-1}, respectively (Fig. 2B and Table 1). We also determined the kinetic parameters of the binding between SLAM or Nectin-4 and MV-H. The ectodomains of SLAM and Nectin-4 were prepared by transient expression in HEK293T cells (Fig. 2A). The kinetic analysis showed the binding affinity of $K_D = 0.17 \pm 0.08$ μM for SLAM (Fig. 2C, Table 1), which is comparable to the previously reported $K_D = 0.41$ μM [7]. On the other hand, the binding constant for Nectin-4 was determined to be $K_D = 0.67 \pm 0.001$ μM (Fig. 2D, Table 1). The K_D value of 2F4-Fab was approximately 9 and 37 times smaller than those of the SLAM and Nectin-4. When the association kinetic constant (k_{on}) to MV-H was compared among 2F4-Fab, SLAM, and Nectin-4, the k_{on} value of 2F4-Fab was roughly 8 times larger than those of SLAM and Nectin-4 (Table 1). On the other hand, the dissociation kinetic constant (k_{off}) of 2F4-Fab was comparable to that of SLAM or approximately 5 times smaller than that of Nectin-4 (Table 1). Consistent with our previous result [13], the 2F4 mAb can inhibit the binding of SLAM to MV-H regardless of the MV strain (Fig. 2E). Those results demonstrate that the 2F4-Fab exhibits sufficient inhibitory activity of the binding of MV-H to both SLAM and Nectin-4.

Next, we designed and prepared scFv, another format of fragmented antibodies of 2F4 mAb. The V_H and V_L encoding regions were cloned into the pGEM-T vector using primer sets summarized in Table 2. The sequences of V_H and V_L were determined and shown with deduced amino acid sequences in Fig. 3A. The sequences of V_H and V_L encode 125 and 104 amino acids, respectively. The complementarity determining regions (CDR) for both V_H and V_L domains were assigned according to the Chothia numbering scheme [22] (http://www.bioinf.org.uk/abs/) (Fig. 3A). The CDR-H2 and

CDR-H3 have 1 and 4 residues' insertion ('S' as H52A for CDR-H2; 'YYAM' as H100A, H100B, H100C and H100D for CDR-H3), respectively, whereas the FR3 of heavy chain contains 3 residues' insertion ('TSL' as H82A, H82B and H82C). When the sequence of the V_H region was analyzed using BLAST, it showed 80% identity to the immunoglobulin (Ig) heavy chain V-III region of Chinese hamsters.

In order to express and purify recombinant 2F4-scFv protein, we have constructed scFvs with different domain orientations, V_H-linker-V_L (HL) and V_L-linker-V_H (LH) since Buhler *et al.* previously reported that the domain orientation of scFv antibody had an impact on its biological activity and productivity [23]. In the present study, the HL scFv showed better inclusion body yield and better refolding efficiency than that of the LH, indicated by the size exclusion chromatography (Fig. 3B and C). Therefore, we used the 2F4-scFv-HL (V_H-V_L orientation) for further experiments, and the protein was designated as 2F4-scFv thereafter. The 2F4-scFv was eluted as a major peak at 190 mL separated by the HiLoad26/60 Superdex75 size exclusion column (Fig. 3B, indicated by arrow). When compared with the molecular size marker indicated on the chromatogram, the molecular mass of the protein was estimated to be 25 kDa by the elution position (Fig. 3C and D), which is in good agreement with that of monomer 2F4-scFv, 26 kDa calculated by the amino acid sequence. The yield of 2F4-scFv was approximately 1.5 mg/L-culture. The purity of the recombinant scFv was >95%, confirmed by SDS-PAGE (Fig. 3E). In addition to the peptide linker of $(GGGGS)_3$, we also examined the different linker sequences, such as GGGGSIAPSMVGGGGS and $(GGGGS)_2$, which have previously improved the affinity and productivity of anti-dinitrophenol and anti-CD20 scFvs [24, 25]. The elution profiles and yields of the scFv with those linker sequences were almost identical to that of $(GGGGS)_3$ linker or even deteriorated (Fig. 3C).

The thermal stabilities of the recombinant 2F4-scFv-HL and 2F4 Fab were analyzed by performing differential scanning calorimetry (DSC) measurements. The DSC curve of 2F4-scFv appeared as a single peak was analyzed by fitting to the none-two state model. The melting temperature midpoint (T_m) for 2F4-scFv was determined to be 49 °C, while the T_m for 2F4 Fab was 76 °C (Fig. 4). The DSC curve indicated that 2F4-scFv and Fab unfold with high cooperativity against heat, suggesting a compact form due to the

relatively stable inter-domain interactions.

To verify whether the 2F4-scFv exhibits functional binding affinity to the MV-H protein, we performed kinetic analyses using SPR. The 2F4-scFv binding was well fitted, and the binding affinity of 2F4-scFv to MV-H was calculated to be K_D = 5.8 ± 1.0 μM (Fig. 5A, Table 1). The K_D values of 2F4-scFv with GGGGSIAPSMVGGGGS and $(GGGGS)_2$ linkers were 5.6 ± 0.05 and 8.9 ± 2 μM, respectively (Fig. 5B and C, Table 1). Since different linker sequences did not alter the binding affinity so far, we used 2F4-scFv with $(GGGGS)_3$ linker hereafter. The K_D value of scFv was approximately 35 and 9 times larger than those of the SLAM and Nectin-4 (Table 1). The k_{on} value of scFv was 0.33 ± 0.05×10^4 M^{-1} s^{-1}, which is roughly 6 times smaller than that of SLAM, whereas the k_{off} value, was 19 ± 0.7×10^{-3} s^{-1}, which is approximately 6 times larger (Fig. 1 and 5, Table 1). On the other hand, the k_{on} value of Nectin-4 was roughly 7 times larger than that of scFv, while the k_{off} values for both scFv and Nectin-4 were comparable (Fig. 1 and 5, Table 1).

We next performed kinetic analysis of the binding between 2F4-scFv and MV-H at five different temperatures, from 10 to 30 °C (283.15 to 303.15 K) (Table 3). The Gibbs free energy change in the binding at each temperature was calculated from the equation 1. Subsequently, these data were fit to the none-linear van't Hoff analysis (equation 2) to determine the thermodynamic parameters at 25 °C (298.15 K) (Fig. 5D). The binding of 2F4-scFv to MV-H showed a moderate free energy change, ΔG of 7.2 ± 1.6 kcal mol^{-1}, characterized by favorable enthalpic change, ΔH and unfavorable entropic change, ΔS (Table 4). The 2F4-scFv binding to MV-H exhibited a large heat capacity change, ΔC_p of ~0.87 ± 0.1 kcal mol^{-1} K^{-1} (Table 4). These data suggest the moderate affinity of 2F4-scFv to MV-H.

Next, we examined whether the scFv can directly inhibit the binding of SLAM and Nectin-4 to the MV-H by using SPR. However, since the SPR analysis above indicated that the binding affinity of 2F4 scFv to MV-H is weaker than those of SLAM and Nectin-4 (Fig. 1 and 5, Table 1), we have tried to saturate with SLAM or Nectin-4 on the MV-H immobilized sensor chip surface. It was, however, difficult to maintain saturated state with either SLAM or Nectin-4 because their MV-H interactions show low affinity with fast kinetics (data not shown). Therefore, we analyzed the binding response

of the scFv in the presence of SLAM or Nectin-4 at the saturated level of concentration. To determine the saturation level of SLAM and Nectin-4 binding to MV-H, the equilibrium binding analysis was performed as shown in Fig. 4. The responses at 70 sec, which reached almost equilibrium binding, were plotted against the analyte concentrations, and the plots were fitted directly to the none-linear 1:1 binding model. In this way, the K_D values for scFv, SLAM and Nectin-4 were estimated 5.9 ± 0.7 μM, 0.40 ± 0.1 μM, and 1.0 ± 0.03 μM, respectively (Fig. 6A-C), which were comparable to those calculated by the kinetic analysis (Fig. 1 and 5, Table 1). The mixture of scFv and SLAM or Nectin-4 was injected over the immobilized MV-H, and the binding responses at equilibrium state with and without receptor were compared. The results showed that the binding responses of scFv rarely increased or did not increase in the presence of 8 μM of SLAM (Fig. 6D, filled circles) or 8 μM of Nectin-4 (Fig. 6E, filled circles), indicating that the binding of scFv competed with both SLAM and Nectin-4. The binding responses were increased in the presence of 10 μM of BSA (Fig. 6F, filled circles) with a similar occurrence without BSA (Fig. 6F, open circles), suggesting the competitive and specific inhibition of scFv. Taken together, the 2F4-scFv has an ability to inhibit the receptor binding *in vitro*, but a sufficient amount may be required to achieve reasonable inhibition.

We examined the effect of the 2F4-scFv on the membrane fusion assessed by cell-to-cell fusion assay using mammalian cell expression vectors. We used 10 μM of scFv for the assay since the competition analysis by SPR suggested the requirement of a sufficient concentration of the scFv. In the absence of antibodies, when H and F proteins were expressed, MV-H and F-mediated syncytia formation was observed in both SLAM and Nectin-4 expressing Vero cells (Fig. 7, left panel). Notably, this syncytium formation was not observed when either H or F protein was not expressed, suggesting that the cell-cell fusion observed in the assay occurs only by the presence of both H and F proteins. The syncytium formation was not observed one day after treatment with 10 μM of 2F4-scFv or 5 μM of mAb 2F4 (Fig. 7A and B, middle and right top panels). Moreover, the inhibition effect lasted for at least 2 days, although the syncytia formation kept progressing in the control cells (Fig. 7A and B, middle and right bottom panels). This result clearly revealed that the 2F4-scFv possesses the ability of the inhibition of the MV-H- and F-mediated membrane fusion.

Discussion

We have previously characterized several neutralizing antibodies against MVs [10, 13]. The 2F4 monoclonal antibody effectively neutralizes the recombinant MV infection of both SLAM and Nectin-4 expressing cells [13]. Here we showed that the 2F4 Fab effectively neutralize MV infection via cellular receptors SLAM and Nectin-4.

Several neutralizing antibodies and the detailed locations of neutralizing epitopes (*I*, *II*, *iv*, *v*, *vi* and *vii*) on the H protein were reported for measles neutralization [9, 10, 13]. Among the epitope regions, the epitope *vii* is thought to be recognized by 2F4 based on the neutralizing experiment using mutant strains [13] and the current study. Previous competitive enzyme-linked immunosorbent assay (ELISA) showed that the mAb 2F4 did not compete for MV binding with the mAbs, including E81, E185, E39, and E103, which are recognizing epitopes *I*, *iv*, *v*, and *vi*, respectively [13]. On the other hand, previously reported mAbs, such as B2, BH26, I-41, 80-II-B2, and 16-DE6, similarly or partially recognize the same epitope *vii* [11, 12, 26-28], which appears to compete with 2F4. Therefore, the use of 2F4 in combination with the mAbs which bind to distinct epitopes would be more effective for measles neutralization.

Here we have characterized the binding kinetics and affinities of the scFv to its antigen, MV-H head domain. The K_D value was determined to be 5.8 μM, which is weaker than those of cellular receptors SLAM (K_D = 0.17 μM) and Nectin-4 (K_D = 0.67 μM). Nevertheless, our competition experiments showed the potential of 2F4-scFv to inhibit the binding of the cellular receptors to MV-H (Fig. 6). The cell-to-cell fusion assay demonstrated that the 2F4-scFv possesses sufficient inhibitory activity of the membrane fusion mediated by both SLAM and Nectin-4 although it is needed at higher concentrations than the intact form (Fig. 7). The results suggest that the 2F4-scFv can directly compete with both receptors upon binding to MV-H. The results are consistent with the previous measles neutralizing experiment showing that 2F4 mAb interferes with the infection of the recombinant MV to both SLAM and Nectin-4 expressing cells [13]. Together with the neutralizing assay using intact antibodies and recombinant MVs as well as the complex structures of MV-H head domain bound to receptors, SLAM and Nectin-4, we have proposed that the receptor-binding sites on the H protein consist of the

common interacting residues and are unshielded by the N-linked sugar moieties [10, 13-16, 29]. Our results in this study suggest that the 2F4 mAb directly recognizes a conserved neutralizing epitope to inhibit the receptor binding.

The K_D value of 2F4-scFv to MV-H binding (5.8 μM) was moderate and got worse as compared to that of 2F4 Fab. The thermodynamic analysis suggested that the relatively moderate ΔH and unfavorable ΔS may account for the moderate binding affinity. The thermodynamic parameters were compared with those of antibodies [30-34] and immune cell receptors [35-37] (Table 4). Among antibodies, the 2F4-scFv exhibited relatively smaller ΔG, but similar level of ΔG with those for binding of cell surface receptors to ligands (5.9-7.2 kcal mol^{-1}) (Table 4). Thus, the binding properties of the 2F4-scFv may be rather similar to those between cell surface receptors and ligands with low affinities. In contrast to the listed interactions, the 2F4-scFv interaction exhibited a relatively large negative heat capacity change (0.87 kcal mol^{-1} K^{-1}). The property is believed to be caused by the conformational changes upon ligand binding, so-called "induced fit" and/or the trapping of water molecules at the binding interface. In addition, the thermal stability analysis showed that 2F4-scFv was less stable by roughly 25 °C in T_m than 2F4 Fab, which is probably responsible for weaker binding reaction of scFv. Taken together, 2F4-scFv has unfavorable thermodynamic nature for binding and conformational stability, which result in the moderate binding affinity.

Although an effective measles vaccine is now available, severe outbreaks still occur even in the people previously vaccinated, in addition to those lacking vaccination [1, 38]. The recent Ebola outbreak in West Africa led to a measles outbreak due to the reduced vaccination as a secondary effect of Ebola [39]. Thus, an MV-specific therapeutic has been expected in addition to promoting proper vaccination. In this study, we produced a fragmented neutralizing antibody maintaining sufficient inhibition activity of receptor-mediated cell-cell fusion. Further investigation to improve its productivity and antigen binding affinity are required for therapeutic use. However, although it is still difficult to provide mAb therapy in developing countries, mAbs and related Fab and scFv may be possible candidates for treatments in developed countries.

Materials and methods

Cells and materials

The hybridoma producing 2F4 monoclonal antibody was established in a previous study [13]. The hybridoma was grown in RPMI medium (Wako) supplemented with 15% fetal calf serum (FCS), at 37 °C with 5% CO_2. For mAb purification, the hybridoma was cultured in RPMI medium without serum. Vero cells were maintained in Dulbecco's Modified Eagle's Medium (DMEM) supplemented with 10% FCS at 37 °C with 5% CO_2. *E. coli* BL21 (DE3) CodonPlus-RIL was purchased from Agilent. Polymerase chain reaction (PCR) primers were synthesized by Eurofins Genomics.

Preparation of intact 2F4 mAb and 2F4 Fab fragment

The mAb 2F4 was also purified from hybridoma as described previously [13]. The 2F4 Fab was prepared using Pierce Fab Preparation Kit (Thermo Scientific). Digestion and purification were performed by following the manufacturer's instruction. Briefly, the mAb 2F4 was applied to the spin column containing papain-immobilized resin, which is preequilibrated with cysteine-containing digestion buffer. For digestion reaction, the column was incubated at 37 °C for 4 hours. The digest was then separated from papain by centrifugation. Subsequently, the digest was applied to a PBS-equilibrated Protein A-immobilized agarose column to capture the Fc fragment as well as undigested full length mAb. The Fab fragment was collected as a flow-through fraction.

Gene cloning and sequence determination

Total RNA was extracted from the 2F4 hybridoma clone using Trizol (Invitrogen). The cDNA was synthesized using a PrimeScript RT-PCR Kit (TaKaRa), then the cDNA as template and the primer sets designed according to the previous report [40] (Table 2) were used to amplify the genes encoding heavy and light chains of antibody variable region. The PCR reaction was performed using *ExTaq* DNA polymerase (TaKaRa) according to the manufacturer's instructions. The amplified products were ligated into pGEM-T vector (Promega). The DNA sequences were determined with ABI3100 (Applied Biosystems).

Construction of the expression vector for scFv

We have constructed the expression vectors for scFvs with both V_H-V_L and V_L-V_H orientations, scFv-HL and scFv-LH, respectively. To construct the scFvs, the splicing overlap extension PCR method [41] via the sequence encoding glycine-serine $(GGGGS)_3$ flexible linker was applied. First, the template cDNAs for variable domains of heavy and light chains in the pGEM-T vectors were amplified by PCR with the following primer pairs summarized in Table 5: VH-Fw and VH-linker0-Rv, VL-linker0-Fw and VL-Rv for scFv-HL with $(GGGGS)_3$ linker, VL-Fw and VL-linker0-Rv, VH-linker0-Fw and VH-Rv for scFv-LH with $(GGGGS)_3$ linker, respectively. Either of the primers contains the sequence for a part of the $(GGGGS)_3$ linker to assemble both variable domains. The two PCR products extracted from agarose gel were linked by another round of PCR. The primer sets of VH-Fw and VL-Rv, or VL-Fw and VH-Rv for HL or LH construct were used, and the PCR reaction was performed using KOD-Plus DNA polymerase (TOYOBO) according to the manufacturer's instructions. The amplified fragments were digested by the restriction enzymes, NdeI and EcoRI, and ligated into the NdeI-EcoRI site of the pET22b vector, designated as 2F4-scFv-HL/pET22b and 2F4-scFv-LH/pET22b, respectively. The DNA sequences were confirmed by DNA sequencing. The 2F4-scFv-HL with GGGGIAPSMVGGGGS and $(GGGGS)_2$ linkers were also constructed in the same way using VH-linker1-Rv and VL-linker1-Fw, or VH-linker2-Rv and VL-linker2-Fw primers in Table 5.

Preparation of recombinant 2F4-scFv

The expression plasmid 2F4-scFv-HL/pET22 or 2F4-scFv-HL/pET22 was introduced into *E. coli* strain BL21 (DE3) CodonPlus-RIL. The transformants were cultured in 2×YT medium with 100 mg/L ampicillin (NacalaiTesque) at 37 °C. When the OD_{600} reached to 0.8-1.0, isopropyl β-d-thiogalactopyranoside (IPTG) (NacalaiTesque) was added for induction, at a final concentration of 1 mM and cultured for an additional 6 hours. After induction, the cells were harvested by centrifugation at 5,000×g for 10 min. The inclusion bodies of scFvs were isolated from the cell pellet by sonication, and were washed repeatedly with Triton wash buffer (50 mM Tris-HCl pH 8.0, 100 mM NaCl, 0.5% Triton X-100). The purified 2F4-scFv inclusion bodies were solubilized in denaturant buffer (50 mM Tris-HCl pH 8.0, 10 mM EDTA, 6 M guanidine HCl). The solubilized protein solution was slowly diluted by addition of ice-cold refolding buffer

(100 mM Tris-HCl, pH 8.0, 2 (mM ethylenediaminetetraacetic acid (EDTA), 0.4 M L-Arginine, 3.73 mM cystamine, 6.37 mM cystamine), to a final protein concentration of 1.5 μM. After incubation for 72 hours at 4 °C, the refolded protein solution was concentrated with a VIVAFLOW50 system (Sartorius). The concentrated sample was dialyzed against the dialysis buffer (20 mM Tris-HCl pH 8.0, 100 mM NaCl, 50 mM L-Arginine). The soluble fraction was separated by centrifugation at 30,000×g for 30 min and was applied onto the size exclusion chromatography, using HiLoad26/60 Superdex75 column (GE Healthcare) with gel filtration buffer (20 mM Tris-HCl pH 8.0, 100 mM NaCl). The fractions containing scFv protein were pooled, concentrated to 1.0 mg/mL. The protein concentration was determined using $A_{280}^{0.1\%} = 2.23$ and the purity was judged by sodium dodecyl sulfate polyacrylamide gel electrophoresis (SDS-PAGE).

Preparation of hemagglutinin and receptor proteins

The soluble head domain of the H protein from Edmonston vaccine strain of MV MV-H and the ectodomain of human SLAM protein (SLAM) were purified using HEK293T cells as described previously [14]. The ectodomain of soluble human Nectin-4 was also purified using HEK293T cells. The expression plasmid was constructed by inserting the DNA fragment encoding Nectin-4 ectodomain (1-333) with C-terminal 6x histidine into pCA7 vector [42], which carries chicken beta actin (CAG) promoter. Protein was secreted into the culture supernatant via authentic signal sequence at N-terminus and purified with 6xHis-tag at C-terminus. Briefly, the plasmid DNA was transfected into HEK293T cells using PEI-max (Polyscience, Inc.) and allow them to maintain for further 3 days. The culture supernatant was subsequently applied to HisTrap column (GE Healthcare). The fractions containing Nectin-4 were pooled and further applied onto the Superdex200 10/300GL column in gel filtration buffer (20 mM Tris-HCl pH 8.0, 150 mM NaCl).

Differential scanning calorimetry (DSC)

The thermal stability of 2F4-scFv was measured using a VP-Capillary DSC system (Marvern) with a cell volume of 0.135 mL. The protein was dissolved in phosphate-buffered saline (PBS) at 0.2 mg/mL (8.4 μM). Measurements were performed

with a temperature range from 20 °C to 90 °C at a scan rate of 60 °C/hour. Data was analyzed using Origin software version 7.0 (OriginLab).

Binding analysis using surface plasmon resonance (SPR)

SPR experiments were performed using BIAcore 3000 (GE Healthcare) at 25 °C. MV-H protein was immobilized on the CM5 sensor chip about 1,000 RU, using amine coupling method. For binding analysis, analyte was dissolved in HBS-P buffer (0.01 M HEPES pH 7.4, 0.15 M NaCl, 0.005% (v/v) Surfactant P20) and 30 μL of the analyte was injected over the immobilized MV-H protein or streptavidin (control) at a flow rate of 25 μL/min. The binding response at each concentration of 2F4-Fab (0.063, 0.13, 0.25, 0.5, and 1.0 μM) was calculated by subtracting the equilibrium response measured in the control flow cell from the response in each sample flow cell. The binding response at each concentration of 2F4-scFv (0.25, 0.5, 1.0, 2.0, 4.0, and 8.0 μM) was calculated by subtracting the equilibrium response measured in the control flow cell from the response in each sample flow cell. For the receptors, human SLAM and Nectin-4, the different concentrations of SLAM (0.094, 0.19, 0.38, 0.75, 1.5, and 3.0 μM) or Nectin-4 (0.11, 0.22, 0.44, 0.88, 1.8, 3.5, and 7.0 μM) was injected over the same chip on which MV-H was immobilized. The kinetic parameters were calculated using the curve-fitting facility of the BIAevaluation version 4.1.1 software (GE healthcare) and the simple 1:1 Langmuir binding model (A + B ↔ AB).

Thermodynamic analyses were performed at five different temperature points, 10, 15, 20, 25, and 30 °C (283.15, 288.15, 293.15, 298.15, and 303.15 K). The standard state Gibbs energy change upon binding was obtained from equation 1;

$$\Delta G = -RT \ln(1/K_{\mathrm{D}}) \qquad (eq\ 1)$$

where K_{D} is the equilibrium dissociation constant, expressed in units of mol/liter, and R is the gas constant. The ΔG values at each temperature point were plotted against the temperatures and were fitted with the none-linear van't Hoff equation (equation 2);

$$\Delta G = \Delta H - T\Delta S + \Delta C_p(T - T_0) - \Delta C_p T \ln(T/T_0) \qquad (eq\ 2)$$

where ΔH and ΔS indicate the binding enthalpy and entropy changes at T_0 = 25 °C (298.15 K), respectively, and ΔC_p is the heat capacity, which is assumed to be temperature-independent.

For the competition assay, the various concentrations of 2F4-scFv were mixed with a fixed concentration of SLAM (8 μM), Nectin-4 (8 μM) or BSA (10 μM), and flowed over the immobilized MV-H protein. The equilibrium binding responses (at 70 sec) were plotted against the concentrations of injected scFvs.

MV neutralizing assay

Neutralizing assay. A suspension of recombinant MV (2,000 PFU per 75 μl) was incubated with serially diluted mAbs for 30 min at 37 °C (the first dilution of each mAb was 1:10, followed by 2-fold dilutions). After incubation with the mAb, the virus solution was inoculated into culture media of confluent monolayers of Vero/Nectin-4 and Vero/ SLAM cells. For recombinant viruses possessing the genotype A H gene (genotype A viruses; IC/EdH-Luci and IC/EdH-EGFP) and their mutants, CD46-dependent infection was blocked by a mAb against CD46 (clone M75) when the assay was performed with II-18 cells. At 2 days post-infection, the luciferase activity in the cells was measured using a Dual-Glo luciferase assay system (Promega). The neutralizing titer was indicated by the maximum dilution point, exhibiting >50% reduction of luciferase activity.

Cell-to-cell fusion assay

Cell-to-cell fusion assay was performed as described previously with slight modification [43]. Briefly, Vero cells stably expressing human SLAM or Nectin-4 (Vero/SLAM [44], Vero/Nectin-4 [43]) were seeded on the 96 well-plate one day before transfection. Transfection was performed using polyethylenimine (PEI) max (Polysciences). MV-H, MV-F, and EGFP expressing plasmids (0.05 ng each; MV-H/ps pCA7 [45], MV-F/pCXN2 [45], and EGFP/pCA7 [46]) were mixed with the 0.30 mg of PEI max and incubated for 20 min. The DNA mixture was then added to the cells. Either 2F4-scFv or full-length antibody was added to the cells 5 hours after transfection. The EGFP expression was observed at the indicated time point using INVERTED SYSTEM MICROSCOPE. IX71 with IX2-RFA Fluorescence Illuminator (ORYMPUS) and the

images were captured using DP2-BSW software (ORYMPUS).

Acknowledgments

We would like to thank Profs. Yusuke Yanagi, Kyushu University, and Shinji Ohno, University of the Ryukyus, for providing mAb 2F4. We would also like to thank Prof. Jun-ichi Miyazaki of Osaka University, for providing CAG promoter containing plasmid vector. This work was supported in part by the Japan Society for the Promotion of Science (JSPS) Grants-in-Aid for Scientific Research KAKENHI (Grants 20057020, and 22121007), JSPS Strategic Young Researcher Overseas Visits Program for Accelerating Brain Circulation, Platform Project for Supporting Drug Discovery and Life Science Research (Basis for Supporting Innovative Drug Discovery and Life Science Research (BINDS)) from AMED under Grant Number 18am0101093j0002, the Platform for Drug Discovery, Informatics, and Structural Life Science, the Ministry of Education, Science, Sports, Culture, and Technology, the Ministry of Health, Labor, and Welfare of Japan, the Japan Bio-oriented Technology Research Advancement Institute (BRAIN), AMED J-PRIDE (Grant Number JP18fm0208022h), Hokkaido University Biosurface Project, Takeda Science Foundation, and the Naito Foundation.

Author Contributions

TT, HF and KM designed this research. TT, MLJ, YI, MT and HF performed experiments, supported by SC, AI, NS, KY, MS, TO and TH. TT, MLJ and TM analyzed the data, supported by MT, HF and KM. TT and MLJ wrote the manuscript with comments from TM, TH, MT, HF and KM.

Conflict of interest

The authors declare that they have no conflicts of interest with the contents of this article.

References

1. Rota, P., Brown, K., Mankertz, A., Santibanez, S., Shulga, S., Muller, C., Hubschen, J., Siqueira, M., Beirnes, J., Ahmed, H., Triki, H., Al-Busaidy, S., Dosseh, A., Byabamazima, C., Smit, S., Akoua-Koffi, C., Bwogi, J., Bukenya, H., Wairagkar, N., Ramamurty, N., Incomserb, P., Pattamadilok, S., Jee, Y., Lim, W., Xu, W., Komase, K., Takeda, M., Tran, T., Castillo-Solorzano, C., Chenoweth, P., Brown, D., Mulders, M., Bellini, W. & Featherstone, D. (2011) Global Distribution of Measles Genotypes and Measles Molecular Epidemiology, *Journal of Infectious Diseases.* **204**, S514-S523.
2. Yanagi, Y., Takeda, M. & Ohno, S. (2006) Measles virus: cellular receptors, tropism and pathogenesis, *Journal of General Virology.* **87**, 2767-2779.
3. Moss, W. & Griffin, D. (2012) Measles, *Lancet.* **379**, 153-164.
4. Tatsuo, H., Ono, N., Tanaka, K. & Yanagi, Y. (2000) SLAM (CDw150) is a cellular receptor for measles virus, *Nature.* **406**, 893-897.
5. Muhlebach, M., Mateo, M., Sinn, P., Prufer, S., Uhlig, K., Leonard, V., Navaratnarajah, C., Frenzke, M., Wong, X., Sawatsky, B., Ramachandran, S., McCray, P., Cichutek, K., von Messling, V., Lopez, M. & Cattaneo, R. (2011) Adherens junction protein nectin-4 is the epithelial receptor for measles virus, *Nature.* **480**, 530-U153.
6. Noyce, R., Bondre, D., Ha, M., Lin, L., Sisson, G., Tsao, M. & Richardson, C. (2011) Tumor Cell Marker PVRL4 (Nectin 4) Is an Epithelial Cell Receptor for Measles Virus, *PLoS Pathogens.* **7**.
7. Hashiguchi, T., Kajikawa, M., Maita, N., Takeda, M., Kuroki, K., Sasaki, K., Kohda, D., Yanagi, Y. & Maenaka, K. (2007) Crystal structure of measles virus hemagglutinin provides insight into effective vaccines, *Proceedings of the National Academy of Sciences of the United States of America.* **104**, 19535-19540.
8. Hashiguchi, T., Fukuda, Y., Matsuoka, R., Kuroda, D., Kubota, M., Shirogane, Y., Watanabe, S., Tsumoto, K., Kohda, D., Plemper, R. & Yanagi, Y. (2018) Structures of the prefusion form of measles virus fusion protein in complex with inhibitors, *Proceedings of the National Academy of Sciences of the United States of America.* **115**, 2496-2501.
9. Sato, T., Fukuda, A. & Sugiura, A. (1985) Characterization of major structural proteins of Measles-virus with monoclonal-antibodies, *Journal of General Virology.* **66**, 1397-1409.
10. Tahara, M., Ito, Y., Brindley, M., Ma, X., He, J., Xu, S., Fukuhara, H., Sakai, K., Komase, K., Rota, P., Plemper, R., Maenaka, K. & Takeda, M. (2013) Functional and Structural Characterization of Neutralizing Epitopes of Measles Virus Hemagglutinin Protein, *Journal of Virology.* **87**, 666-675.
11. Bouche, F., Ertl, O. & Muller, C. (2002) Neutralizing B cell response in measles,

Viral Immunology. **15**, 451-471.
12. Ertl, O., Wenz, D., Bouche, F., Berbers, G. & Muller, C. (2003) Immunodominant domains of the Measles virus hemagglutinin protein eliciting a neutralizing human B cell response, *Archives of Virology.* **148**, 2195-2206.
13. Tahara, M., Ohno, S., Sakai, K., Ito, Y., Fukuhara, H., Komase, K., Brindley, M., Rota, P., Plemper, R., Maenaka, K. & Takeda, M. (2013) The Receptor-Binding Site of the Measles Virus Hemagglutinin Protein Itself Constitutes a Conserved Neutralizing Epitope, *Journal of Virology.* **87**, 3583-3586.
14. Hashiguchi, T., Ose, T., Kubota, M., Maita, N., Kamishikiryo, J., Maenaka, K. & Yanagi, Y. (2011) Structure of the measles virus hemagglutinin bound to its cellular receptor SLAM, *Nature Structural & Molecular Biology.* **18**, 135-U191.
15. Zhang, X., Lu, G., Qi, J., Li, Y., He, Y., Xu, X., Shi, J., Zhang, C., Yan, J. & Gao, G. (2013) Structure of measles virus hemagglutinin bound to its epithelial receptor nectin-4, *Nature Structural & Molecular Biology.* **20**, 67-U86.
16. Santiago, C., Celma, M., Stehle, T. & Casasnovas, J. (2010) Structure of the measles virus hemagglutinin bound to the CD46 receptor, *Nature Structural & Molecular Biology.* **17**, 124-U152.
17. Tahara, M., Burckert, J., Kanou, K., Maenaka, K., Muller, C. & Takeda, M. (2016) Measles Virus Hemagglutinin Protein Epitopes: The Basis of Antigenic Stability, *Viruses-Basel.* **8**.
18. Pelegrin, M., Naranjo-Gomez, M. & Piechaczyk, M. (2015) Antiviral Monoclonal Antibodies: Can They Be More Than Simple Neutralizing Agents?, *Trends in Microbiology.* **23**, 653-665.
19. Buss, N., Henderson, S., McFarlane, M., Shenton, J. & de Haan, L. (2012) Monoclonal antibody therapeutics: history and future, *Current Opinion in Pharmacology.* **12**, 615-622.
20. Nelson, A. (2010) Antibody fragments Hope and hype, *Mabs.* **2**, 77-83.
21. Holliger, P. & Hudson, P. (2005) Engineered antibody fragments and the rise of single domains, *Nature Biotechnology.* **23**, 1126-1136.
22. AlLazikani, B., Lesk, A. & Chothia, C. (1997) Standard conformations for the canonical structures of immunoglobulins, *Journal of Molecular Biology.* **273**, 927-948.
23. Buhler, P., Wetterauer, D., Gierschner, D., Wetterauer, U., Beile, U. & Wolf, P. (2010) Influence of Structural Variations on Biological Activity of Anti-PSMA scFv and Immunotoxins Targeting Prostate Cancer, *Anticancer Research.* **30**, 3373-3379.
24. Turner, D., Ritter, M. & George, A. (1997) Importance of the linker in expression of single-chain Fv antibody fragments: Optimisation of peptide sequence using phage

display technology, *Journal of Immunological Methods.* **205**, 43-54.
25. Gu, X., Jia, X., Feng, J., Shen, B., Huang, Y., Geng, S., Sun, Y., Wang, Y., Li, Y. & Long, M. (2010) Molecular Modeling and Affinity Determination of scFv Antibody: Proper Linker Peptide Enhances Its Activity, *Annals of Biomedical Engineering.* **38**, 537-549.
26. Sheshberadaran, H. & Norrby, E. (1986) Characterizaiton of epitopes on the Measles-virus hemagglutinin, *Virology.* **152**, 58-65.
27. Hu, A., Sheshberadaran, H., Norrby, E. & Kovamees, J. (1993) Molecular characterization of epitopes on the Measles-virus hemagglutinin protein, *Virology.* **192**, 351-354.
28. Hummel, K. & Bellini, W. (1995) Localization of monoclonal-antibody epitopes and functional domains in the hemagglutinin protein of Measles-virus, *Journal of Virology.* **69**, 1913-1916.
29. Hashiguchi, T., Maenaka, K. & Yanagi, Y. (2011) Measles virus hemagglutinin: structural insights into cell entry and measles vaccine, *Frontiers in Microbiology.* **2**.
30. Acierno, J., Braden, B., Klinke, S., Goldbaum, F. & Cauerhff, A. (2007) Affinity maturation increases the stability and plasticity of the Fv domain of anti-protein antibodies, *Journal of Molecular Biology.* **374**, 130-146.
31. Kiyoshi, M., Caaveiro, J., Miura, E., Nagatoishi, S., Nakakido, M., Soga, S., Shirai, H., Kawabata, S. & Tsumoto, K. (2014) Affinity Improvement of a Therapeutic Antibody by Structure-Based Computational Design: Generation of Electrostatic Interactions in the Transition State Stabilizes the Antibody-Antigen Complex, *PLoS One.* **9**.
32. Schwarz, F., Tello, D., Goldbaum, F., Mariuzza, R. & Poljak, R. (1995) Themrmodynamics of antigen-antibody binding using specific anti-lysozyme antibodies, *European Journal of Biochemistry.* **228**, 388-394.
33. Makabe, K., Nakanishi, T., Tsumoto, K., Tanaka, Y., Kondo, H., Umetsu, M., Sone, Y., Asano, R. & Kumagai, I. (2008) Thermodynamic consequences of mutations in Vernier zone residues of a humanized anti-human epidermal growth factor receptor murine antibody-528, *Journal of Biological Chemistry.* **283**, 1156-1166.
34. Crespillo, S., Casares, S., Mateo, P. & Conejero-Lara, F. (2014) Thermodynamic Analysis of the Binding of 2F5 (Fab and Immunoglobulin G Forms) to Its gp41 Epitope Reveals a Strong Influence of the Immunoglobulin Fc Region on Affinity, *Journal of Biological Chemistry.* **289**, 594-599.
35. Shiroishi, M., Kuroki, K., Tsumoto, K., Yokota, A., Sasaki, T., Amano, K., Shimojima, T., Shirakihara, Y., Rasubala, L., van der Merwe, P., Kumagai, I., Kohda, D. & Maenaka, K. (2006) Entropically driven MHC class I recognition by human inhibitory

receptor leukocyte Ig-like receptor B1 (LILRB1/ILT2/CD85j), *Journal of Molecular Biology.* **355**, 237-248.
36. Maenaka, K., Juji, T., Nakayama, T., Wyer, J., Gao, G., Maenaka, T., Zaccai, N., Kikuchi, A., Yabe, T., Tokunaga, K., Tadokoro, K., Stuart, D., Jones, E. & van der Merwe, P. (1999) Killer cell immunoglobulin receptors and T cell receptors bind peptide-major histocompatibility complex class I with distinct thermodynamic and kinetic properties, *Journal of Biological Chemistry.* **274**, 28329-28334.
37. Kamishikiryo, J., Fukuhara, H., Okabe, Y., Kuroki, K. & Maenaka, K. (2011) Molecular Basis for LLT1 Protein Recognition by Human CD161 Protein (NKRP1A/KLRB1), *Journal of Biological Chemistry.* **286**, 23823-23830.
38. Rota, P., Brown, K., Hubschen, J., Muller, C., Icenogle, J., Chen, M., Bankamp, B., Kessler, J., Brown, D., Bellini, W. & Featherstone, D. (2011) Improving Global Virologic Surveillance for Measles and Rubella, *Journal of Infectious Diseases.* **204**, S506-S513.
39. Takahashi, S., Metcalf, C., Ferrari, M., Moss, W., Truelove, S., Tatem, A., Grenfell, B. & Lessler, J. (2015) Reduced vaccination and the risk of measles and other childhood infections post-Ebola, *Science.* **347**, 1240-1242.
40. Imai, S., Mukai, Y., Nagano, K., Shibata, H., Sugita, T., Abe, Y., Nomura, T., Tsutsumi, Y., Kamada, H., Nakagawa, S. & Tsunoda, S. (2006) Quality enhancement of the non-immune phage scFv library to isolate effective antibodies, *Biological & Pharmaceutical Bulletin.* **29**, 1325-1330.
41. Horton, R., Cai, Z., Ho, S. & Pease, L. (1990) Gene-splicing by overlap extension - Tailor-made genes using the polymerase chain-reaction, Biotechniques. 8, 528-535.
42. Niwa, H., Yamamura, K. & Miyazaki, J. (1991) Efficient selection for high-expression transfectants with a novel eukaryotic vector, *Gene.* **108**, 193-199.
43. Otsuki, N., Sekizuka, T., Seki, F., Sakai, K., Kubota, T., Nakatsu, Y., Chen, S., Fukuhara, H., Maenaka, K., Yamaguchi, R., Kuroda, M. & Takeda, M. (2013) Canine distemper virus with the intact C protein has the potential to replicate in human epithelial cells by using human nectin4 as a receptor, *Virology.* **435**, 485-492.
44. Ono, N., Tatsuo, H., Hidaka, Y., Aoki, T., Minagawa, H. & Yanagi, Y. (2001) Measles viruses on throat swabs from measles patients use signaling lymphocytic activation molecule (CDw150) but not CD46 as a cellular receptor, *Journal of Virology.* **75**, 4399-4401.
45. Tahara, M., Takeda, M., Shirogane, Y., Hashiguchi, T., Ohno, S. & Yanagi, Y. (2008) Measles virus infects both polarized epithelial and immune cells by using distinctive receptor-binding sites on its hemagglutinin, *Journal of Virology.* **82**, 4630-4637.
46. Komune, N., Ichinohe, T., Ito, M. & Yanagi, Y. (2011) Measles Virus V Protein

Inhibits NLRP3 Inflammasome-Mediated Interleukin-1 beta Secretion, *Journal of Virology.* **85**, 13019-13026.

Figure legends

Figure 1: Effect of the neutralizing antibody on the MV infection. (A) Preparation of the antibody and its fragment. SDS-PAGE of the purified proteins; Lane1, Marker; lane2, full length 2F4 mAb, lane3, 2F4 Fab. (B) MV neutralizing assay. Relative MV infection as a function of the antibody concentration is shown for Vero/SLAM cells (left) and Vero/Nectin-4 cells. Open circle indicates the 2F4 mAb, whereas filled circle indicates the 2F4 Fab. Error bars represent ± SD.

Figure 2: Kinetic analyses of 2F4 Fab, SLAM, or Nectin-4 with MV-H immobilized on the sensor chip. (A) Preparation of the recombinant proteins. SDS-PAGE of (left) purified MV-H; Lane1, Marker; lane2, MV-H head domain, (middle) purified human SLAM; Lane1, Marker; lane2, human SLAM ectodomain, (right) purified human Nectin-4; Lane1, Marker; lane2, human Nectin-4 ectodomain. Small dashed line between the lanes that have been spliced together to generate the figures are indicated on the gel images for MV-H and SLAM. (B-D) Representative sensorgrams for the binding between MV-H and Fab or cellular receptors. 2F4 Fab (B), SLAM (C), and Nectin-4 (D) at different concentrations were injected over the immobilized MV-H from Edomonstone strain (MV-H(Ed)), and the representative sensorgrams are shown. Response curves were fitted by the simple 1:1 Langmuir binding model. The thick black line indicates actual response curves, whereas the thin red line indicates the fitting curves. The kinetic parameters are summarized in Table 1. Experiments were repeated at least three times. (E) Blocking analysis between MV-H and SLAM using SPR. Cyan broken line indicates sensorgram of SLAM injected over the immobilized MV-H from wild type (WT) strain (MV-H(WT)), blue line indicates that over the immobilized MV-H(WT) saturated with 2F4 mAb, pink broken line indicates that over the immobilized MV-H(Ed), red line indicates that over the immobilized MV-H(Ed) saturated with 2F4 mAb.

Figure 3: Purification of the recombinant 2F4-scFv protein. (A) The amino acid sequence of the V_H and V_L domains of 2F4 mAb. The CDRs are boxed off. The insertion amino acid residues are shown in bold with orange. (B) Comparison between scFv-HL and scFv-

LH. Recombinant scFvs were expressed in *E. coli* as inclusion bodies for both scFv-HL (left) and scFv-LH (right). Lane1, Marker; lane2, before induction; lane 3, after induction; lane4, supernatant; lane5, inclusion body. (C) Chromatogram of the size exclusion chromatography for scFv-HL with $(GGGGS)_3$ linker (thick blue line), that with GGGGIAPSMVGGGGS linker (broken cyan line), that with $(GGGGS)_2$ linker (thin dark blue line) and for scFv-LH with $(GGGGS)_3$ linker (thick red line). Black arrow indicates the elution position of the scFv. (D) Standard curve for the size exclusion chromatography. The filled circles indicate the position of the protein standard, whereas the open rhomboid indicates the position of the major peak of the chromatogram for scFv-HL (the black line in C, indicated by arrow). The equation and R-square value of the fitting were indicated on the graph. (E) SDS-PAGE with Coomassie staining. Lane 1, molecular size marker; lane 2, 2 μg of purified 2F4-scFv.

Figure 4: Thermal stability of 2F4-scFv and 2F4 Fab. Orange line indicates the thermogram of 2F4-scFv, whereas brown line indicates that of 2F4 Fab. Protein was dissolved in PBS at 0.2 mg/mL and DSC measurements were performed at a scan rate of 60 °C/h. The DSC curve was fitted to the none-two state unfolding model.

Figure 5: Kinetic analyses of 2F4-scFv with MV-H immobilized on the sensor chip. Representative sensorgrams for the binding responses between MV-H and (A) 2F4-scFv with $(GGGGS)_3$ linker, (B) 2F4-scFv with GGGGIAPSMVGGGGS linker or (C) 2F4-scFv with $(GGGGS)_2$ linker. 2F4-scFv at different concentrations were injected over the immobilized MV-H and the representative sensorgrams are shown. Response curves were fitted by the simple 1:1 Langmuir binding model. The thick black line indicates actual response curves, whereas the thin red line indicates the fitting curves. The kinetic parameters are summarized in Table 1. Experiments were repeated at least three times. (D) Thermodynamic analysis of the binding of 2F4-scFv to immobilized MV-H. The SPR experiments were performed at five different temperatures (283.15 - 303.15 K) and the free energy (ΔG) the enthalpic (ΔH) and standard entropic ($-T\Delta S$) changes at 25 °C (298.15 K) and the specific heat capacity (ΔC_p) for binding were determined by fitting the equation 2 to these data.

Figure 6: The effect of SLAM or Nectin-4 on the binding of the 2F4-scFv to MV-H. The equilibrium binding of scFv (A), SLAM (B), and Nectin-4 (C) to MV-H. The responses of equilibrium binding at 70 sec in Figure 3 were plotted against each analyte concentration. The solid lines indicate direct nonlinear fits of the 1:1 binding model. (D) Binding of 2F4-scFv in the absence (open blue circles) or presence (filled red circles) of 8 μM hSLAM. (E) Binding of 2F4-scFv in the absence (open blue circles) or presence (filled red circles) of 8 μM Nectin-4. (F) Binding of 2F4-scFv in the absence (open blue circles) or presence (filled red circles) of 10 μM BSA.

Figure 7: Effect of 2F4-scFv and intact 2F4 on the membrane fusion. The assay is based on the co-transfection of Vero cells with plasmids expressing H protein, F protein, and GFP. The images were captured 24 h and 48 h after transfection, and the representative images are shown for SLAM-expressing Vero cells (A) and Nectin-4-expressing Vero cells (B). Two biological independent experiments were performed.

Table 1: Kinetic parameters of the binding to MV-H

Analyte	K_D (μM)	k_{on} ($\times 10^4$, M^{-1} s^{-1})	k_{off} ($\times 10^{-3}$, s^{-1})	K_D^{eq} (μM)
2F4-Fab	0.018 ± 0.003	17 ± 1	2.8 ± 0.3	—
2F4-scFv $(GGGGS)_3$ linker	5.8 ± 1	0.33 ± 0.05	19 ± 0.7	5.9 ± 0.7
2F4-scFv GGGGIAPSMVGGGGS linker	5.6 ± 0.05	0.34 ± 0.03	19 ± 1	—
2F4-scFv $(GGGGS)_2$ linker	8.9 ± 2	0.23 ± 0.01	20 ± 3	—
SLAM	0.17 ± 0.08	2.0 ± 0.6	3.0 ± 0.4	0.40 ± 0.1
SLAM*	0.41	1.1	4.5	—
Nectin-4	0.67 ± 0.001	2.3 ± 0.2	15 ± 0.2	1.0 ± 0.03

The analyte was injected over the immobilized MV-H protein. The kinetic parameters of binding were calculated by the fitting with the simple 1:1 Langmuir binding model. The equilibrium dissociation constant, K_D values were calculated with the equation $K_D = k_{off}/k_{on}$. The χ^2 values for the Fab, scFv with $(GGGGS)_3$ linker, GGGGIAPSMVGGGGS linker, $(GGGGS)_2$ linker, SLAM and Nectin-4 were 4.4, 5.5, 4.6, 4.3, 2.1 and 14 respectively.

Apparent equilibrium dissociation constant K_D^{eq} values were calculated as shown in Fig. 6A-C. *Kinetic parameters are referred from Hashiguchi et al. 2007 [7].

Table 2: Primer sequences for V_H and V_L cloning.

	Forward primer name	Sequence	Reverse primer name	Sequence
VL region	VL-F1	5′-CCGAYATTGTWCTCWCCCARTC-3′	VL-R1	5′-CCGTTTGATTTCCARCTTKG-3′
	VL-F2	5′-CCGAYATTSTGMTSACYCAGTC-3′	VL-R2	5′-CCGTTTTATTTCCAGCTTGG-3′
	VL-F3	5′-CCGAYATTGTGMTMACTCAGTC-3′	VL-R3	5′-CCGTTTSAGCTCCAGCTTGG-3′
	VL-F4	5′-CCGAYATTGTGHTRWCACAGTC-3′	VL-R4	5′-CCGTTYWATTTCCAACTTWG-3′
	VL-F5	5′-CCGAYATTGTRATGACMCAGTC-3′	VL-R5	5′-CCCTAGGACAGTCAGTTTGG-3′
	VL-F6	5′-CCGAYATTMAGATRAMCCAGTC-3′		
	VL-F7	5′-CCGAYATTCAGATGAYDCAGTC-3′		
	VL-F8	5′-CCGAYATTTTGCTGACTCAGTC-3′		
	VL-F9	5′-CCGAYATTGTTCTCAWCCAGTC-3′		
	VL-F10	5′-CCGAYATTGWGCTSACCCAATC-3′		
	VL-F11	5′-CCGAYATTSTRATGACCCARTC-3′		
	VL-F12	5′-CCGAYRTTKTGATGACCCAVAC-3′		
	VL-F13	5′-CCGAYATYCAGATGACACAGAC-3′		
	VL-F14	5′-CCGAYATTGTGATGACACAACC-3′		
	VL-F15	5′-CCGAYATCCAGCTGACTCAGCC-3′		
	VL-F16	5′-CCGAYATTGTGATGACBCAGKC-3′		
	VL-F17	5′-CCGAYATTGTGATAACYCAGGA-3′		
	VL-F18	5′-CCGAYATTGTGATGACCCAGWT-3′		
	VL-F19	5′-CCGAYGTGSTGMTSACYCAGTC-3′		
	VL-F20	5′-CCGAYGCTGTTGTACTCAGGAATC-3′		
	VL-F21	5′-CCGAYATTGTDHTVWCHCAGTC-3′		
VH region	VH-F1	5′-CCGAKGTRMAGCTTCAGGAGYC-3′	VH-R1	5′-GCYGAGGAAACGGTGACCGTGGT-3′
	VH-F2	5′-CCGAGGTNCAGCTBCAGCAGTC-3′	VH-R2	5′-GCYGAGGAGACTGTGAGAGTGGT-3′
	VH-F3	5′-CCCAGGTGCAGCTGAAGSASTC-3′	VH-R3	5′-GCYGAGGAGACGGTGACTGAGRT-3′
	VH-F4	5′-CCCAGSTBCAGCTGCAGCAGTC-3′	VH-R4	5′-GCYGAGGAAGACTGTAGAGTGGT-3′
	VH-F5	5′-CCGAGGTYCAGCTYCAGCAGTC-3′	VH-R5	5′-GCYGCGGAGACASTGACCAGAGT-3′
	VH-F6	5′-CCGARGTCCARCTGCAACARTC-3′	VH-R6	5′-GCYGCAGAGACASTGACCAGAGT-3′
	VH-F7	5′-CCCAGGTYCAGCTBCAGCARTC-3′		
	VH-F8	5′-CCCAGGTYCARCTKCAGCAGTC-3′		
	VH-F9	5′-CCCAGGTCCACGTGAAGCAGTC-3′		
	VH-F10	5′-CCGAGGTGAASSTGGTGGARTC-3′		
	VH-F11	5′-CCGAVGTGAWGYTGGTGGAGTC-3′		
	VH-F12	5′-CCGAGGTGAAGGTCATCGAGTC-3′		
	VH-F13	5′-CCSAGGTGCAGSKGGTGGAGTC-3′		
	VH-F14	5′-CCGAKGTGCAMCTGGTGGAGTC-3′		
	VH-F15	5′-CCGAAGTGCAVCTGGTGGAGTC-3′		
	VH-F16	5′-CCGAGGTGAAGCTGATGGARTC-3′		
	VH-F17	5′-CCGAGGTGCARCTTGTTGAGTC-3′		
	VH-F18	5′-CCGARGTRAAGCTTCTCGAGTC-3′		
	VH-F19	5′-CCGAAGTGAARSTTGAGGAGTC-3′		
	VH-F20	5′-CCGAAGTGATGCTGGTGGAGTC-3′		
	VH-F21	5′-CCCAGGTTACTCTRAAAGWGTSTG-3′		
	VH-F22	5′-CCCAGGTCCAAYTVCAGCARCC-3′		
	VH-F23	5′-CCGATGTGAACTTGGAAGTGTC-3′		

Primer sets were designed that allowed immunoglobulin genes to be amplified as efficiently as possible by referring previous report [40].
S=G/C, R=G/A, K=G/T, M=A/C, Y=C/T, W=A/T, H=A/C/T, B=C/G/T, V=A/C/G, D=A/G/T, N=A/T/G/C

Table 3; kinetic parameters at different temperatures.

Temperature (°C)	K_D (μM)	k_{on} ($\times 10^4$, M^{-1} s^{-1})	k_{off} ($\times 10^{-3}$, s^{-1})
10	5.0 ± 0.2	0.082 ± 0.04	4.1 ± 0.4
15	4.4 ± 0.2	0.16 ± 0.01	7.1 ± 0.03
20	5.0 ± 0.1	0.20 ± 0.02	10 ± 0.3
25*	5.6 ± 0.05	0.34 ± 0.03	19 ± 1
30	7.9 ± 0.2	0.42 ± 0.01	33 ± 0.1

*The data at 25 °C is the same as shown in the Table 1

The kinetic parameters of binding were calculated by the fitting with the simple 1:1 Langmuir binding model. The equilibrium dissociation constant, K_D values were calculated with the equation $K_D = k_{off}/k_{on}$. The χ^2 values for 10 to 30 °C were 0.61, 5.2, 7.7, 5.5 and 10 respectively.

Table 4: Summary of the thermodynamic parameters of the protein binding at 25 °C

Protein	K_D (M)	ΔG (kcal mol^{-1})	ΔH (kcal mol^{-1})	$-T\Delta S$ (kcal mol^{-1})	ΔC_p (kcal mol^{-1} K^{-1})	References
2F4-scFv	$5.8 \pm 1 \times 10^{-6}$	−7.2 ± 1.6	−8.3 ± 0.6	1.1 ± 0.6	−0.87 ± 0.1	current study
antibody						
anti-lysozyme Fv	0.1×10^{-9}	−13.6	−18.2	−4.6	—	Acierno JP *et al*. 2007 [30]
anti-MCP-1[a] scFv	0.8×10^{-9}	−12.5	−7.3	−5.0	—	Kiyoshi M *et al*. 2014 [31]
anti-lysozyme Fab	1.4×10^{-9}	−12.0	−11.0	−1.0	—	Schwarz FP *et al*. 1995 [32]
anti-EGFR Fv	53×10^{-9}	−9.9	−14.6	4.7	−0.34	Makabe K *et al*. 2008 [33]
anti-HIV-1 Fab[b]	50×10^{-9}	−9.9	−17.2	7.3	—	Crespillo S *et al*. 2014 [34]
Cell surface receptor						
LILRB1–MHC-I	8.1×10^{-6}	−6.8	−0.2	−6.6	−0.16	Shiroishi M *et al*. 2006 [35]
KIR2DL3–MHC-I	9.0×10^{-6}	−7.2	−4.1	−3.1	−0.1	Maenaka K *et al*. 1999 [36]
LLT1–CD161	48×10^{-6}	−5.9	−3.2	−2.7	−0.41	Kamishikiryo J *et al*. 2011 [37]

Thermodynamic parameters at the equilibrium state of the binding were calculated using equation 2 at T_0 = 298.15 K (25 °C)

[a] MCP-1; monocyte chemo-attractant protein-1

[b] Thermodynamic parameters were determined by ITC.

Table 5: PCR primers for the construction of scFv expression vectors.

Name	Sequence	Restriction site
For HL		
VH-Fw	5′-GCGAAGACGTACATATGGAGGTGCAGCTGGTGGAG-3′	NdeI
VH-linker0-Rv	5′-*GGATCCACCACCTCCACTGCCGCCACCACCAGACCCACCGCCGCC*TGGTGTCGTTTTGGCTGAGG-3′	
VL-linker0-Fw	5′-*GGCGGCAGTGGAGGTGGTGGATCC*ACACAGACTCCAGCCTCCC-3′	
VH-linker1-Rv	5′-*ACTGCCACCGCCACCCACCATAGAAGGCGCAATCCCACCGCCGCC*TGGTGTCGTTTTGGCTGAGG-3′	
VL-linker1-Fw	5′-*ATTGCGCCTTCTATGGTGGGTGGCGGTGGCAGT*ACACAGACTCCAGCCTCCC-3′	
VH-linker2-Rv	5′-TCTGTGT*ACTGCCGCCACCACCAGACCCACCGCCGCC*TGGTGTCGTTTTGGCTGAGG-3′	
VL-linker2-Fw	5′-*TGGGTCTGGTGGTGGCGGCAGT*ACACAGACTCCAGCCTCCC-3′	
VL-Rv	5′-GCGGAATTCTTACCGTTTGATTTCCAG-3′	EcoRI
For LH		
VL-Fw	5′-CATTCATATGACACAGACTCCAGCCT-3′	NdeI
VL-linker-Rv	5′-*GGATCCACCACCTCCACTGCCGCCACCACCAGACCCACCGCCGCC*CCGTTTGATTTCCAGCTTGG-3′	
VH-linker-fw	5′-*GGCGGCAGTGGAGGTGGTGGATCC*GAGGTGCAGCTGGTGGAGTCTGGG -3′	
VH-Rv	5′-GCGGAATTCTTATGGTGTCGTTTTGGC-3′	EcoRI

Linker1,linker1 and linker2 encode (GGGGS)x3, GGGGIAPSMVGGGGS and (GGGGS)x2, respectively.
Underlined sequence indicates restriction site.
Italic sequence indicates flexible linker region encoding GGGGS repeat or GGGGIAPSMVGGGGS.

Figure 1

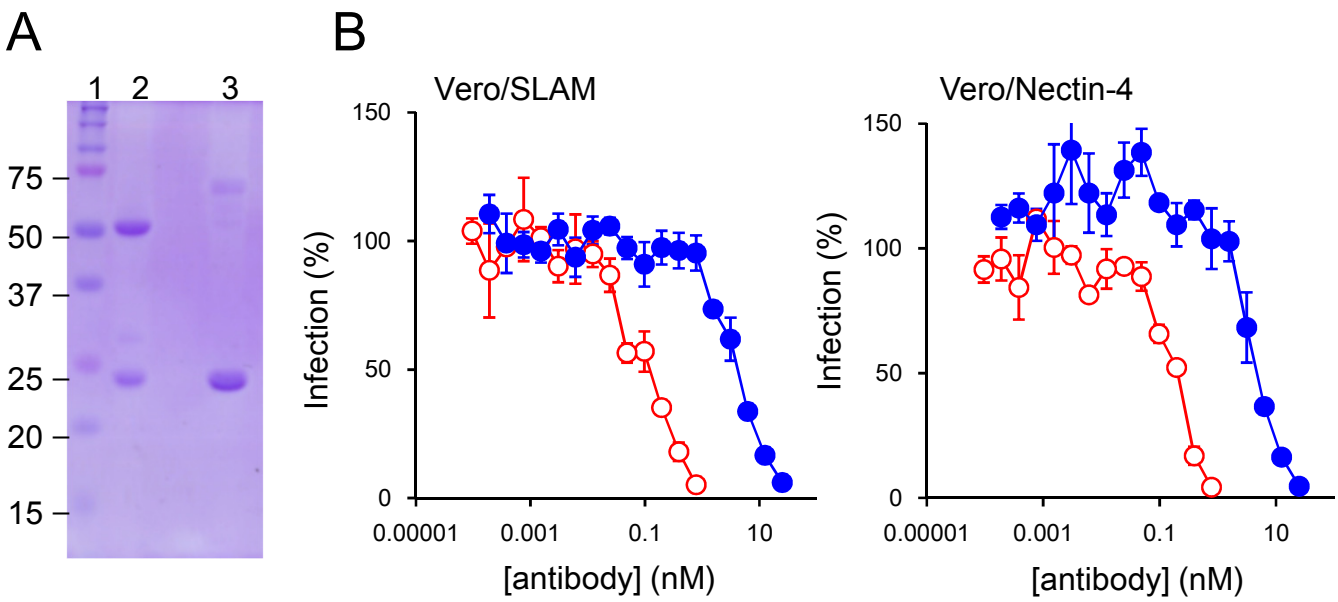
A
1
2
3
75
50
37
25
20
15
B
Vero/SLAM
Vero/Nectin-4
Infection (%)
150
100
50
0
0.00001
0.001
0.1
10
[antibody] (nM)

Figure 2

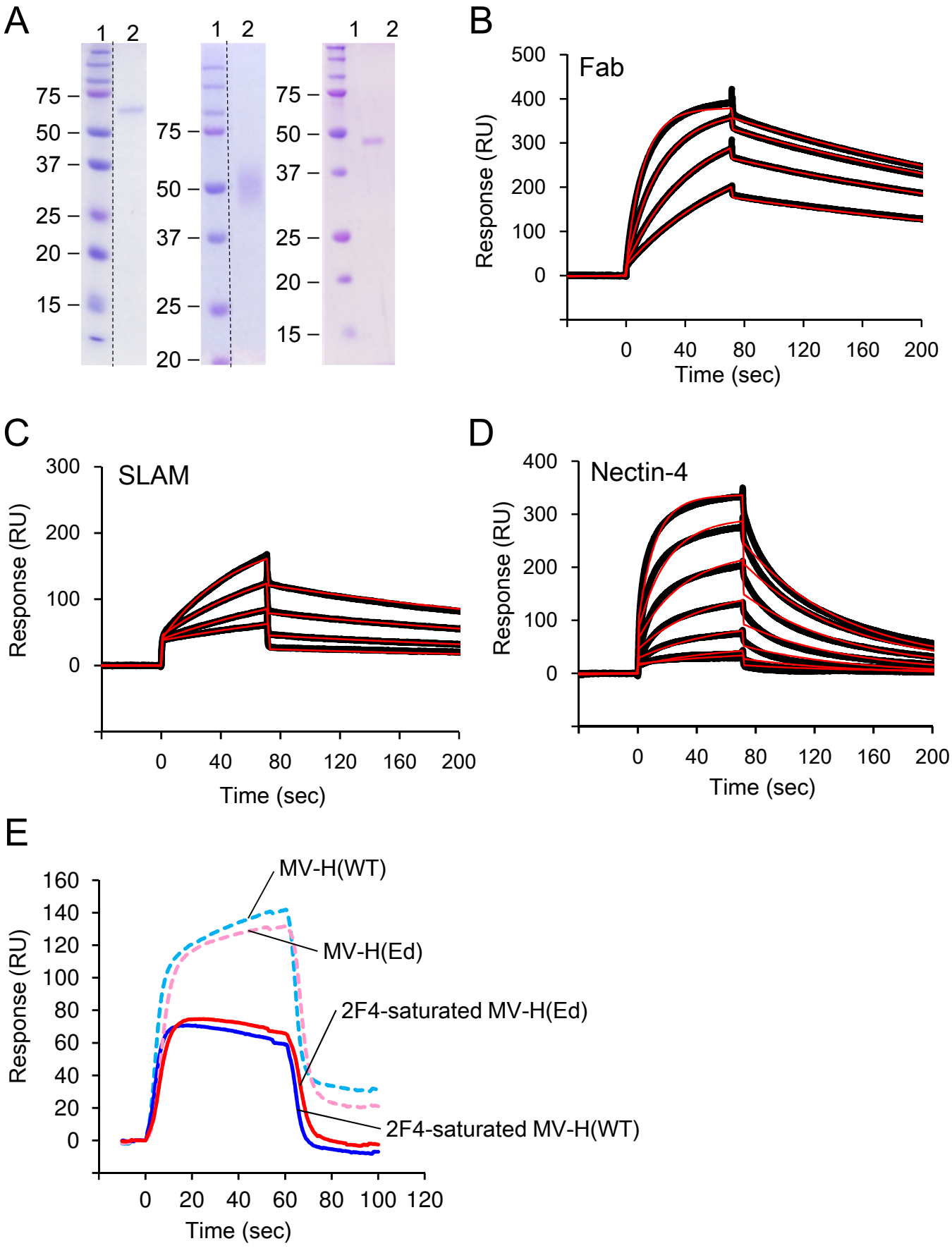
A
1 2
75
50
37
25
20
15
1 2
75
50
37
25
20
1 2
75
50
37
25
20
15
B
Fab
Response (RU)
500
400
300
200
100
0
0 40 80 120 160 200
Time (sec)
C
SLAM
Response (RU)
300
200
100
0
0 40 80 120 160 200
Time (sec)
D
Nectin-4
Response (RU)
400
300
200
100
0
0 40 80 120 160 200
Time (sec)
E
MV-H(WT)
MV-H(Ed)
2F4-saturated MV-H(Ed)
2F4-saturated MV-H(WT)
Response (RU)
160
140
120
100
80
60
40
20
0
0 20 40 60 80 100 120
Time (sec)

Figure 3

A

V_H

EVQLVESGGGLVKPGGSLKLSCAASGFTFSDYGMHWVRQAPEKGLEWVAY

CDR-H1

ISSGSSTIYYADTVKGRFTISRDNAKNTLFLQMTSLRSEDTAMYYCARKG

CDR-H2

YYGLYYAMDYWGQGTSVTVSSAKTTP

CDR-H3

V_L

TQTPASLSVSVGETVTITCRASENIYSNLAWYQQKQGKSPQLLVYAATNL

CDR-L1 CDR-L2

ADGVPSRFSGSGSGTQYSLKINSLQSEDFGSYYCQHFWGTPWTFGGGTKL

CDR-L3

EIKR

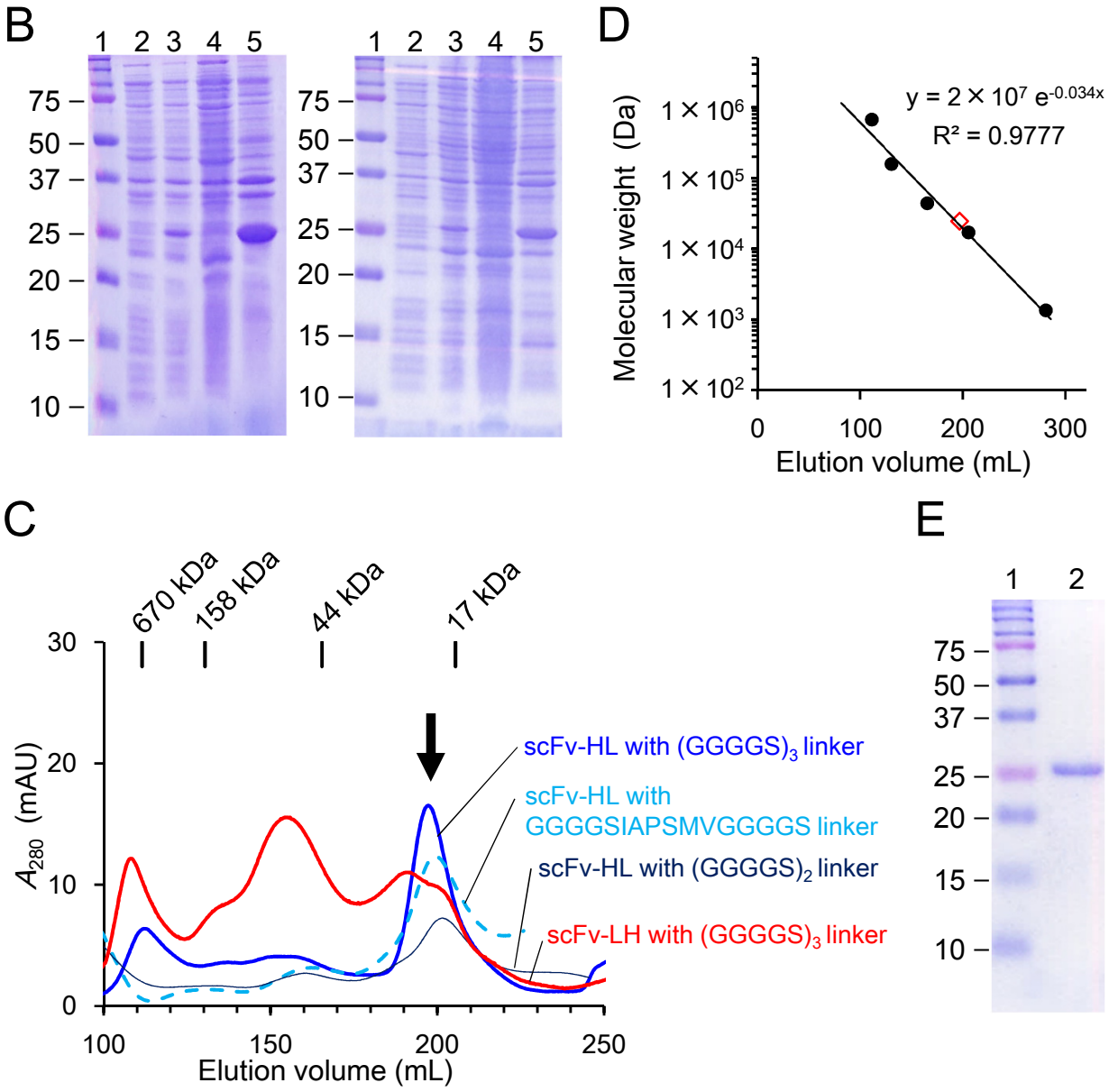

Figure 4

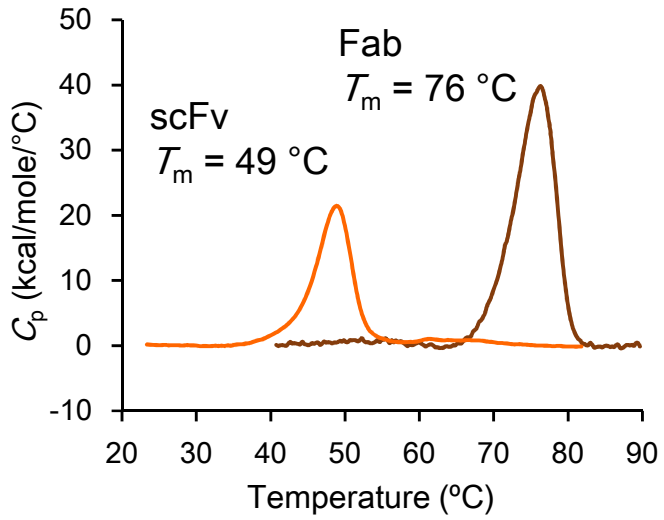
Fab
T_m = 76 °C
scFv
T_m = 49 °C
C_p (kcal/mole/°C)
50
40
30
20
10
0
-10
20
30
40
50
60
70
80
90
Temperature (ºC)

Figure 5

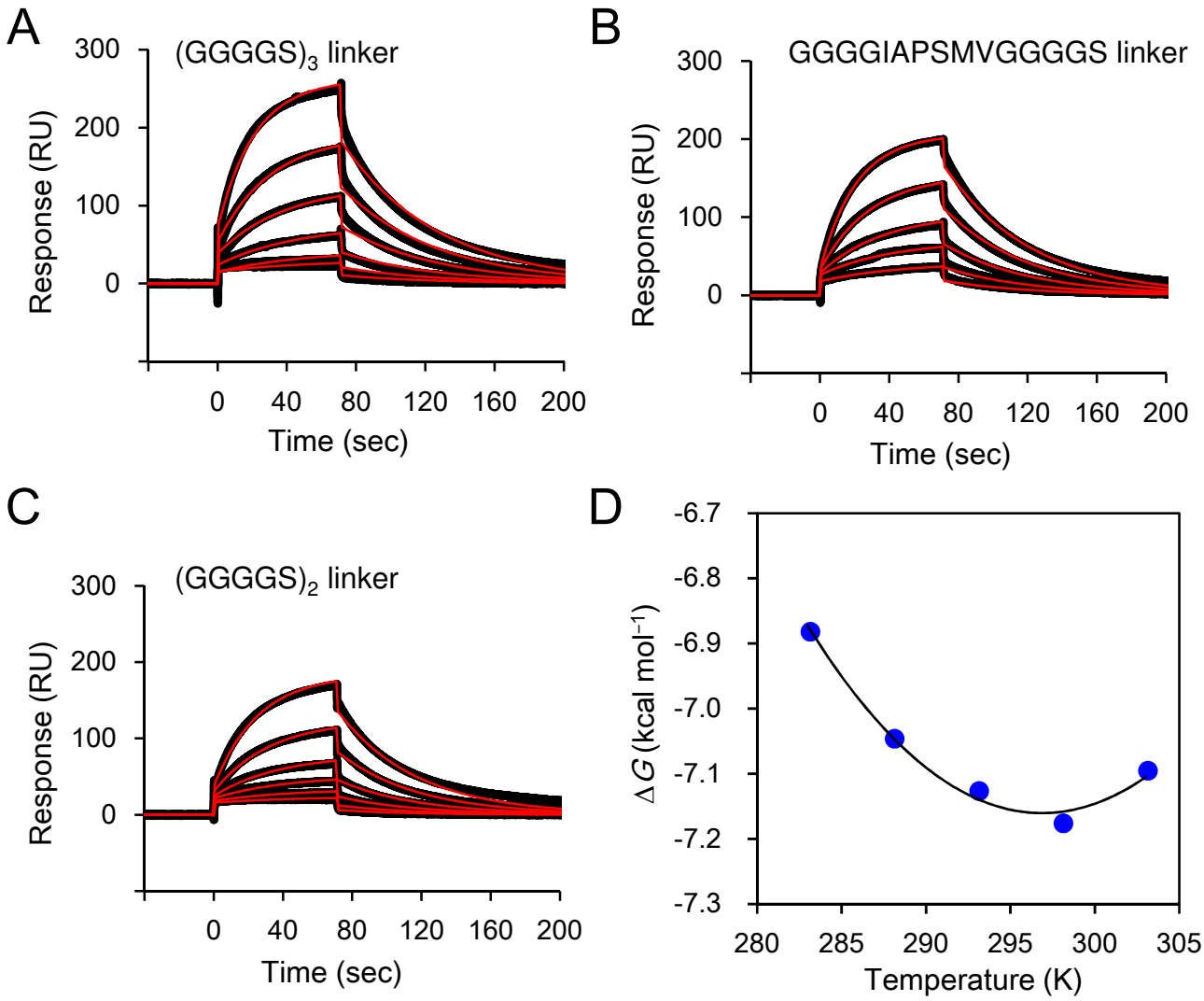
A
(GGGGS)3 linker
Response (RU)
300
200
100
0
0
40
80
120
160
200
Time (sec)
B
GGGGIAPSMVGGGGS linker
Response (RU)
300
200
100
0
0
40
80
120
160
200
Time (sec)
C
(GGGGS)2 linker
Response (RU)
300
200
100
0
0
40
80
120
160
200
Time (sec)
D
ΔG (kcal mol−1)
-6.7
-6.8
-6.9
-7.0
-7.1
-7.2
-7.3
280
285
290
295
300
305
Temperature (K)

Figure 6

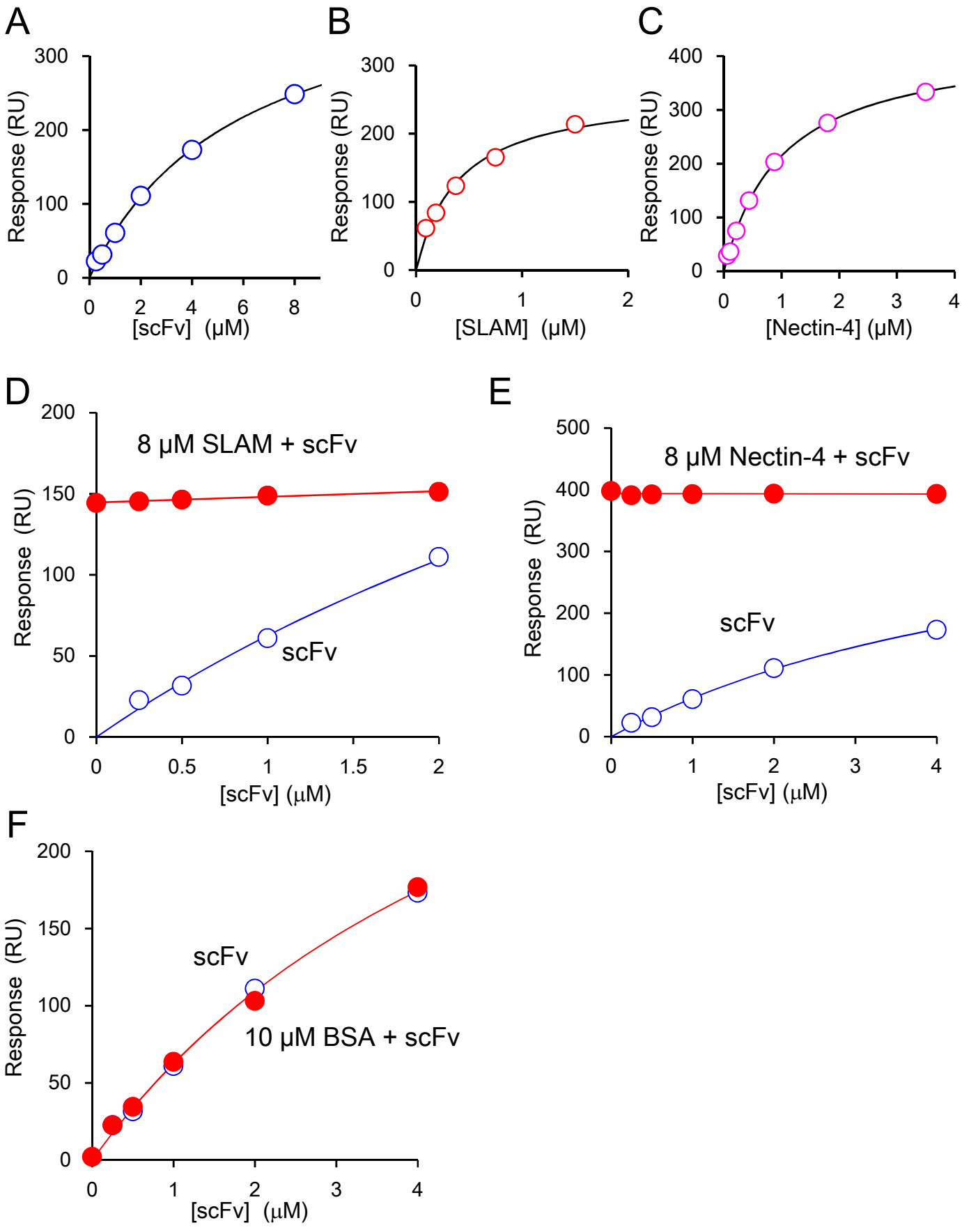
A
Response (RU)
300
200
100
0
0
2
4
6
8
[scFv] (μM)
B
Response (RU)
300
200
100
0
0
1
2
[SLAM] (μM)
C
Response (RU)
400
300
200
100
0
0
1
2
3
4
[Nectin-4] (μM)
D
8 μM SLAM + scFv
scFv
Response (RU)
200
150
100
50
0
0
0.5
1
1.5
2
[scFv] (μM)
E
8 μM Nectin-4 + scFv
scFv
Response (RU)
500
400
300
200
100
0
0
1
2
3
4
[scFv] (μM)
F
scFv
10 μM BSA + scFv
Response (RU)
200
150
100
50
0
0
1
2
3
4
[scFv] (μM)

Figure 7

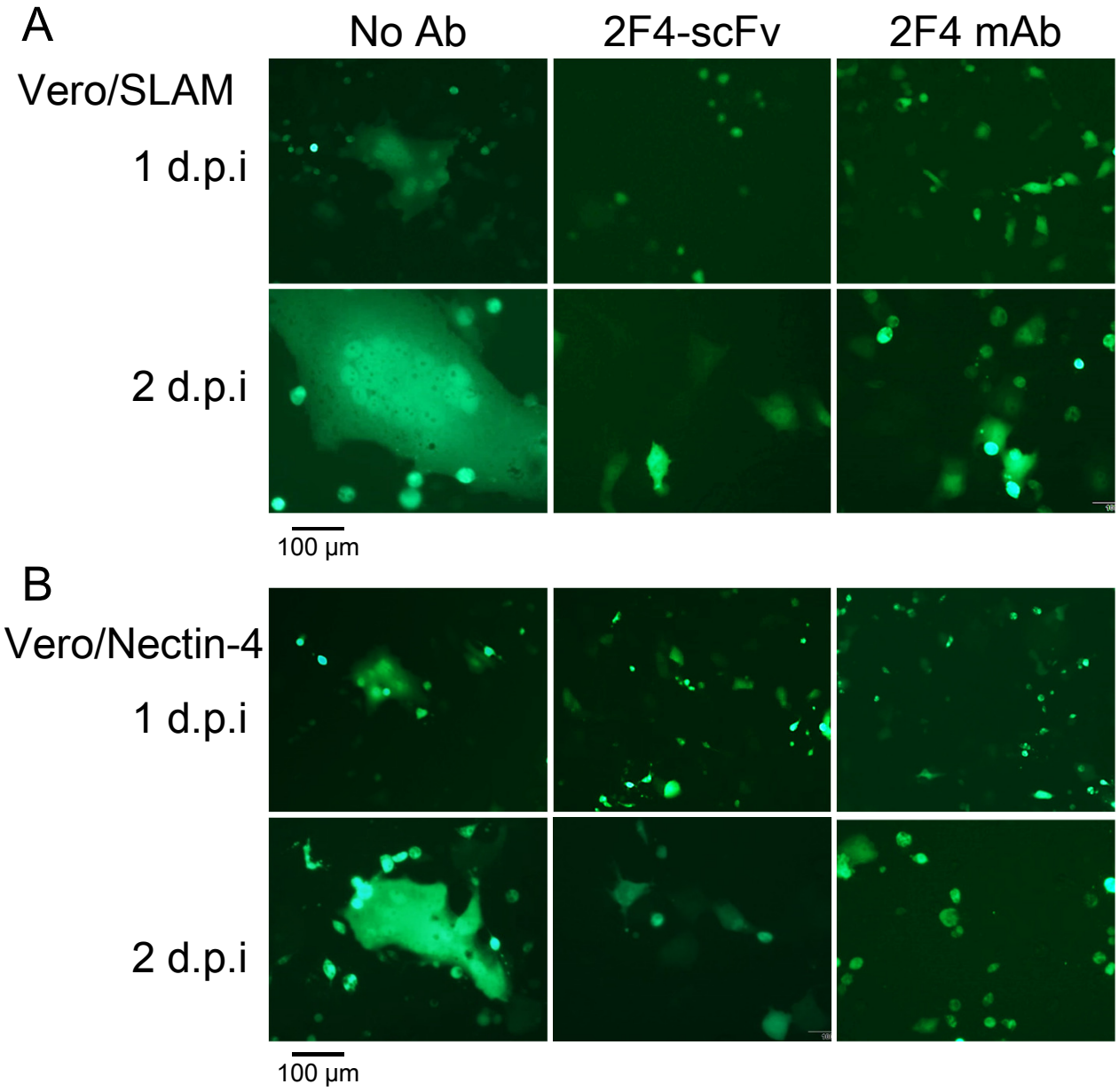
A
No Ab
2F4-scFv
2F4 mAb
Vero/SLAM
1 d.p.i
2 d.p.i
100 μm
B
Vero/Nectin-4
1 d.p.i
2 d.p.i
100 μm